

Large Molecular Gas Reservoirs in Ancestors of Milky Way-Mass Galaxies 9 Billion Years Ago

C. Papovich^{1,2}, I. Labbé³, K. Glazebrook⁴, R. Quadri^{1,2}, G. Bekiaris⁴, M. Dickinson⁵, S. L. Finkelstein⁶, D. Fisher⁴, H. Inami^{5,7}, R. C. Livermore⁶, L. Spitler^{8,9}, C. Straatman³, K.-V. Tran^{1,2}

The gas accretion and star-formation histories of galaxies like the Milky Way remain an outstanding problem in astrophysics.^{1,2} Observations show that 8 billion years ago, the progenitors to Milky Way-mass galaxies were forming stars 30 times faster than today and predicted to be rich in molecular gas,³ in contrast with low present-day gas fractions (<10%).⁴⁻⁶ Here we show detections of molecular gas from the CO($J=3-2$) emission (rest-frame 345.8 GHz) in galaxies at redshifts $z=1.2-1.3$, selected to have the stellar mass and star-formation rate of the progenitors of today's Milky Way-mass galaxies. The CO emission reveals large molecular gas masses, comparable to or exceeding the galaxy stellar masses, and implying most of the baryons are in cold gas, not stars. The galaxies' total luminosities from star formation and CO luminosities yield long gas-consumption timescales. Compared to local spiral galaxies, the star-formation efficiency, estimated from the ratio of total IR luminosity to CO emission, has remained nearly constant since redshift $z=1.2$, despite the order of magnitude decrease in gas fraction, consistent with results for other galaxies at this epoch.⁷⁻¹⁰ Therefore the physical processes that determine the rate at which gas cools to form stars in distant galaxies appear to be similar to that in local galaxies.

Studies of the distribution of stellar ages and elemental abundances in the Milky Way and M31 conclude most of their stars formed in the distant past, more than 7 billion years ago.^{11,12} This agrees with recent work that shows star-formation in present-day galaxies with the mass of the Milky Way peaked more than 8 billion years ago, at $z>1$,³ with star-formation rates (SFRs) exceeding $30 M_{\odot} \text{ yr}^{-1}$, compared to a present-day SFR of $1.7 \pm 0.2 M_{\odot} \text{ yr}^{-1}$ for the Milky Way.¹³

(<10%) at redshifts $z\sim 1$.²⁰ Others predict that the gas flows from the IGM can perturb and disrupt the formation of disk instabilities, thereby suppressing star formation in galaxies and extending star-formation histories.^{21,22} The first step to understand star formation in galaxies like the Milky Way is to measure the amount of the cold gas in their progenitors at $z>1$. As the gas is the fuel for star formation, the ratio of the SFR to gas mass can test the physical processes in the models.²³

With the greatly improved sensitivity offered by the Atacama Large Millimeter Array (ALMA), we are able now to explore the evolution of cold molecular gas in low mass galaxies at redshifts $z > 1$. With ALMA, we observed the $J=3$ to 2 transition of CO in four galaxies with the stellar mass and SFR expected of the main progenitors to present-day Milky Way-mass galaxies at redshifts $z = 1.2 - 1.3$ selected from deep imaging by the FourStar Galaxy Evolution (ZFOURGE) survey²⁴ (see discussion in the Methods). Figure 1 shows the integrated emission from the CO $J = 3$ to 2 transition in these galaxies, where the detections range in significance from 4.8–13.7 σ (r.m.s.). The CO(3–2) emission coincides with the spatial positions of the galaxies in Hubble Space Telescope (HST) imaging (Figure 1); the small offsets are consistent with astrometric calibrations and ALMA beam smearing. Table 1 gives the measured properties of these galaxies. The ALMA detections of CO emission probe the molecular mass in galaxies with the stellar mass and SFRs that the main progenitor of the Milky Way was expected to have ~ 8.5 billion years ago. This provides an important extension of previous work, as the galaxies in our sample have lower stellar masses and SFRs than have been generally possible to study at these redshifts.¹⁰

- Не ясна ситуация с формированием дисков в галактиках с $M^* \sim 10^{10} M_{\odot}$: потоки холодной аккреции не дают SF быстро затухнуть .
- ПРОБЛЕМА: эволюция холодного газа на $Z > 1$.
- Наблюдения: CO(3-2) (ALMA) + HST imaging+L_IR (8-1000 μm (Spitzer+Herschel))

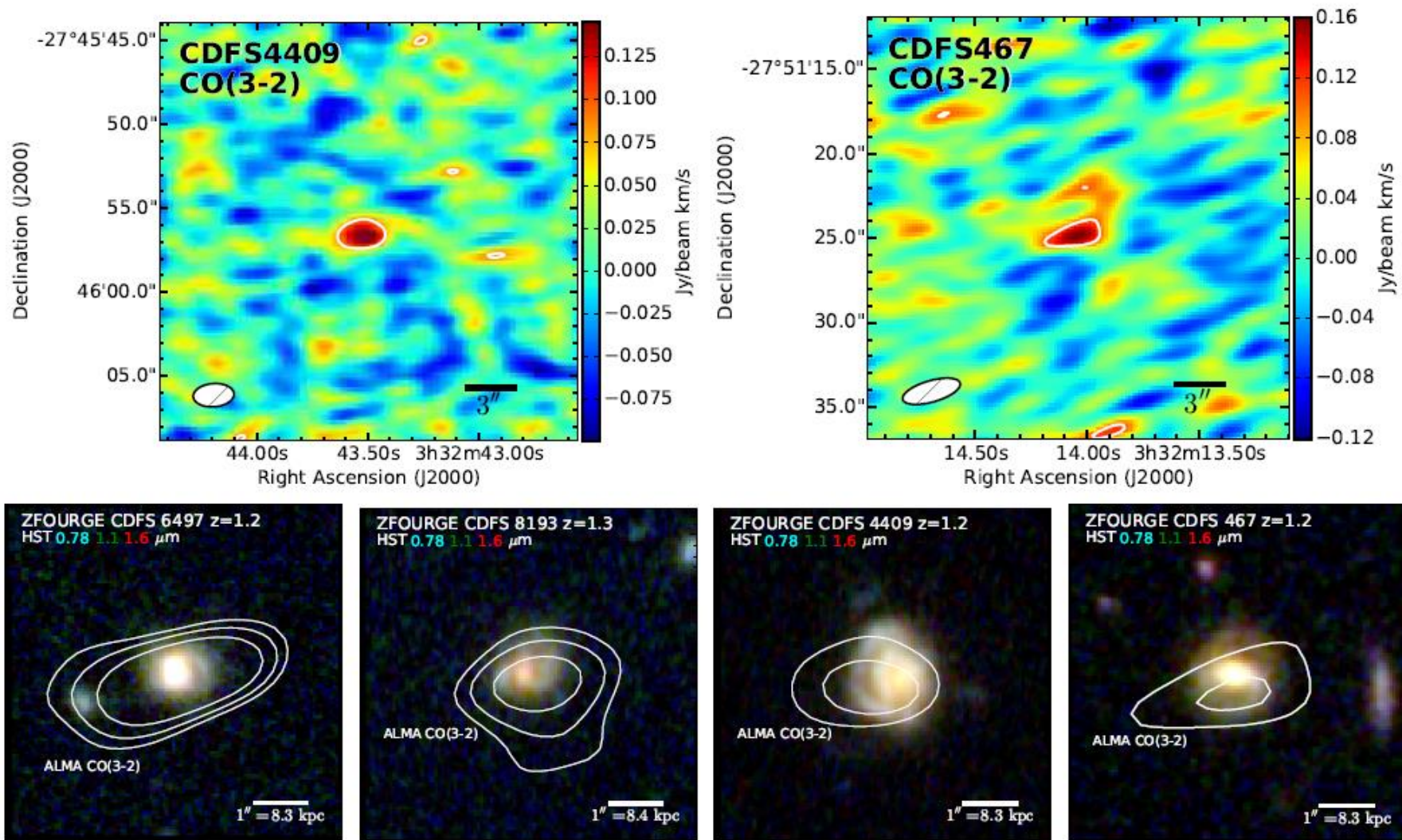
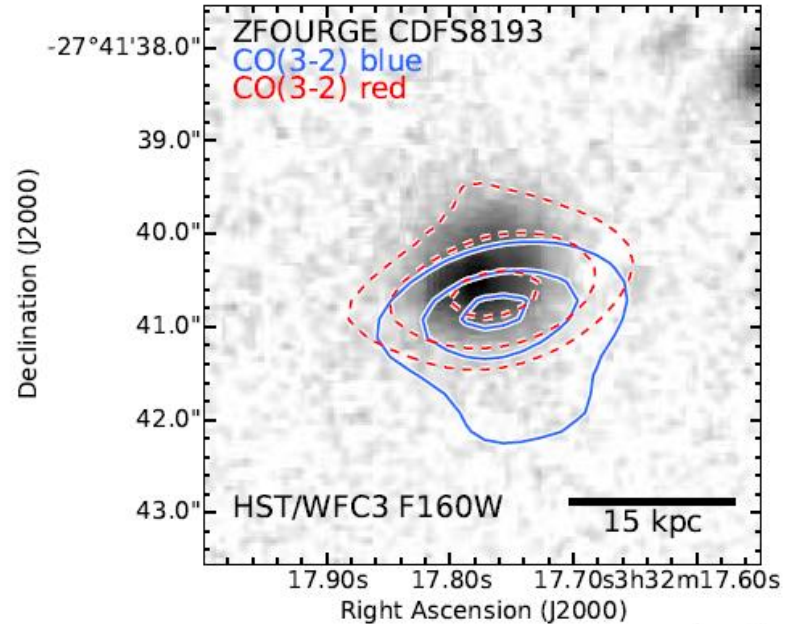
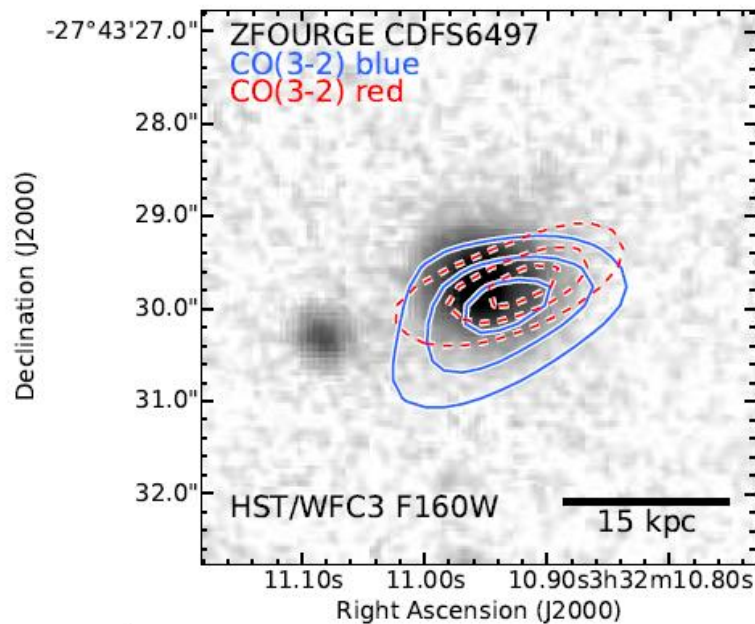


Figure 1 | Images of Milky Way Progenitors at redshifts $z = 1.2$ to 1.3 . The top panels show the ALMA images of the redshifted CO $J=3-2$ emission for each galaxy. The inset bar shows a scale length of 3 arcseconds, and the hashed ellipse shows the size of the synthesized ALMA beam of each observation. The contours denote the emission at 2 times the noise. The bottom panels show combined Hubble Space Telescope images at 0.78, 1.1, and 1.6 μm (approximately the rest-frame U -, V -, and R -band emission). The contours denote ALMA CO(3-2) emission with levels at 2, $2\sqrt{2}$, and 4 times the noise. The inset bar shows a scale length of 1 arcsecond, which corresponds to a physical scale of 8.3–8.4 kpc at these redshifts.



Supplementary Figure 4 | CO(3–2) maps of two galaxies with velocity shear: spatial offsets in their velocity components. The contours show the CO(3–2) emission from the blue-shifted (approaching) and red-shifted (receding) emission. The contours are overdrawn on the HST/WFC3 F160W images from CANDELS.^{36,37}

- Признаки вращения?

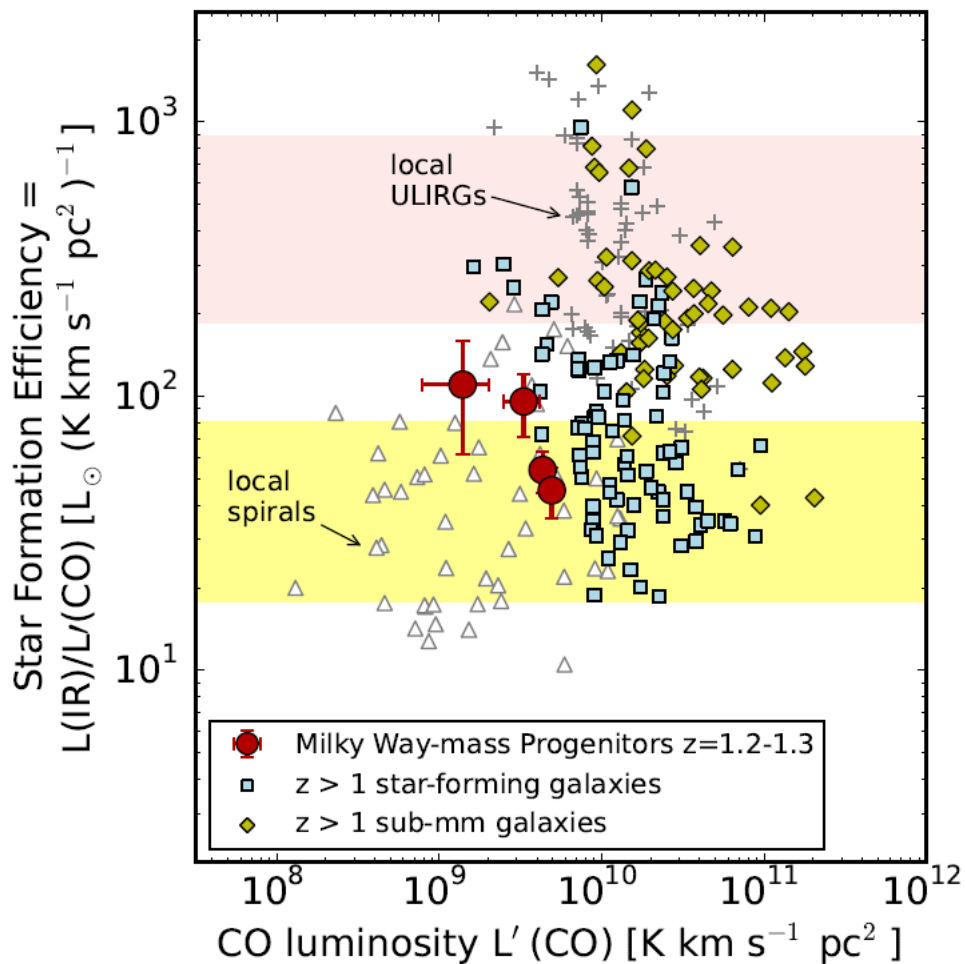


Figure 2 | Star Formation Efficiency as a function of CO luminosity, $L'(\text{CO})$. The star-formation efficiency is defined as the ratio of the total IR luminosity (L_{IR}) to $L'(\text{CO})$, where $L'(\text{CO})$ is converted to the emission of the $J=1-0$ transition. The $z = 1.2 - 1.3$ galaxies in our sample are shown as large red circles. Error bars denote 1σ uncertainties. Other small symbols denote control samples of star-forming galaxies, including local spiral galaxies (open triangles), local ultraluminous IR galaxies (ULIRGs; crosses),²⁹⁻³¹ high redshift ($z > 1$) star-forming galaxies (cyan-filled squares), and high redshift submillimetre galaxies (yellow-filled diamonds).^{10,32} The shaded regions show the interquartile ranges of the star-formation efficiency for local normal spirals and ULIRGs.

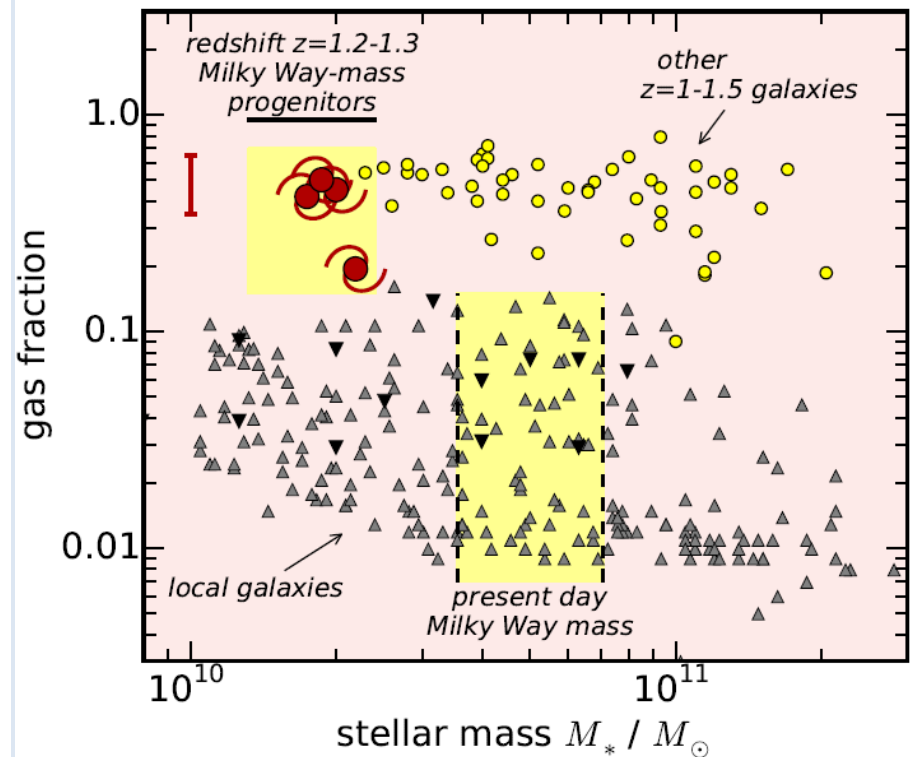


Figure 3 | The relation between the molecular gas fraction and total stellar mass in galaxies at $z = 1 - 1.5$ compared to local galaxies. Here the gas fraction is defined as the ratio $M_{\text{gas}}/(M_{\text{gas}} + M_*)$. The progenitors of Milky Way-mass galaxies at $z = 1.2 - 1.3$ are denoted by large, red spirals. The red bar shows the typical statistical uncertainty, $\approx 30\%$. Smaller, yellow circles show other galaxies at $z = 1 - 1.5$.^{7,9,10} The smaller triangles show measurement for local ($z \sim 0$) galaxies with data from the literature, including COLD GASS (gray, upward triangles) and the HERA CO line excitation survey⁵ (black, downward triangles). The region separated by vertical dashed lines shows the stellar mass range of Milky Way-like galaxies at present.

Время исчерпания CO-газа – 200-700 Myr
(мало отличается от современных галактик)

Выводы

- Высокая $M_{\text{molgas}}/(M_{\text{molgas}}+M^*) > 0.5$ на $z \sim 1$ - против модели с быстрым расходом газа на SF и требует аккреции $\sim > 6 \text{ Ms/yr}$.
- За время от $z=1$ до $z=0$ барионная масса галактик могла вырасти лишь на 30 – 50%, чему соответствует $\text{SFR} \sim 1-2 \text{ Ms/yr}$ (аккреция значительна только первые неск. Млрд лет истории).

Тонкое место: насколько верен фактор конверсии?

Gas and stellar spiral arms and their offsets in the grand-design spiral galaxy M51

Fumi Egusa^{1,2*}, Erin Mentuch Cooper³, Jin Koda⁴, and Junichi Baba^{5,6}

¹*Institute of Space and Astronautical Science, Japan Aerospace Exploration Agency, Sagamihara, Kanagawa 252-5210, Japan*

²*Chile Observatory, National Astronomical Observatory of Japan, Mitaka, Tokyo 181-8588, Japan*

³*Department of Astronomy, The University of Texas at Austin, Austin, TX 78712-1205, USA*

⁴*Department of Physics and Astronomy, Stony Brook University, Stony Brook, NY 11794-3800, USA*

⁵*Earth-Life Science Institute, Tokyo Institute of Technology, Meguro-ku, Tokyo 152-8550, Japan*

⁶*Research Center for Space and Cosmic Evolution, Ehime University, Matsuyama, Ehime 790-8577, Japan*

Last updated : in original form

ABSTRACT

Theoretical studies on the response of interstellar gas to a gravitational potential disc with a quasi-stationary spiral arm pattern suggest that the gas experiences a sudden compression due to standing shock waves at spiral arms. This mechanism, called a galactic shock wave, predicts that gas spiral arms move from downstream to upstream of stellar arms with increasing radius inside a corotation radius. In order to investigate if this mechanism is at work in the grand-design spiral galaxy M51, we have measured azimuthal offsets between the peaks of stellar mass and gas mass distributions in its two spiral arms. The stellar mass distribution is created by the spatially resolved spectral energy distribution fitting to optical and near infrared images, while the gas mass distribution is obtained by high-resolution CO and HI data. For the inner region ($r \leq 150''$), we find that one arm is consistent with the galactic shock while the other is not. For the outer region, results are less certain due to the narrower range of offset values, the weakness of stellar arms, and the smaller number of successful offset measurements. The results suggest that the nature of two inner spiral arms are different, which is likely due to an interaction with the companion galaxy.

Key words: galaxies: individual (M51 or NGC5194) – galaxies: spiral – galaxies: structure

1 INTRODUCTION

The nature of stellar and gaseous spiral arms in galactic discs has been studied about 50 years and is still being discussed actively. In

ral potential, is called galactic shock wave theory. In the case of tightly wound stellar spiral arms, Woodward (1975) presented that the galactic shocks appear within a few 100 Myr. This result sug-

- Теоретические предсказания.
- Многочисленные попытки найти радиус коротации по азимутальному сдвигу между газом и SF (по $H\alpha$)
- Оценки R_{cor} по разным работам:
- 2.1'; 2.9'; 5'; 1.5'; совсем нет коротации.

- В настоящей работе:
- А) рассматривается сдвиг между максимумом поверхностной плотности звезд (используя SED, opt+IR) и газа (CO+HI).
- Б) отдельно рассматриваются arm 1, arm 2, внешние и внутренние ветви

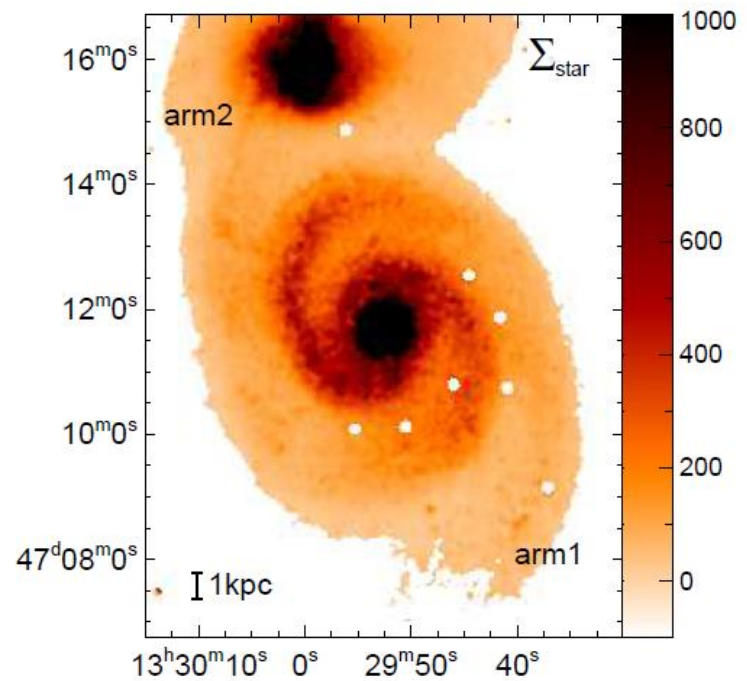
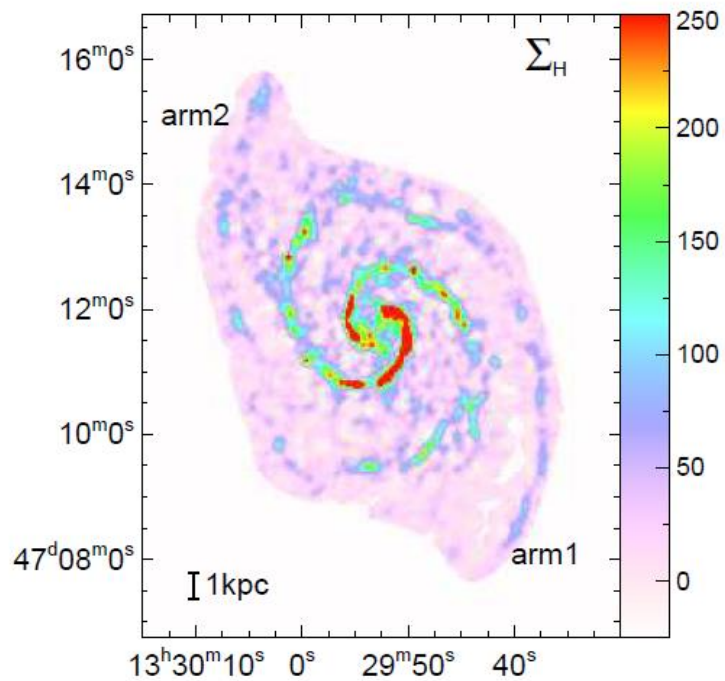


Figure 1. Smoothed and regridded images of Σ_H (left) and Σ_{star} (right) of M51. The coordinates are right ascension and declination (J2000), and the unit of the colour scale is [M_{\odot}/pc^2] for both images.

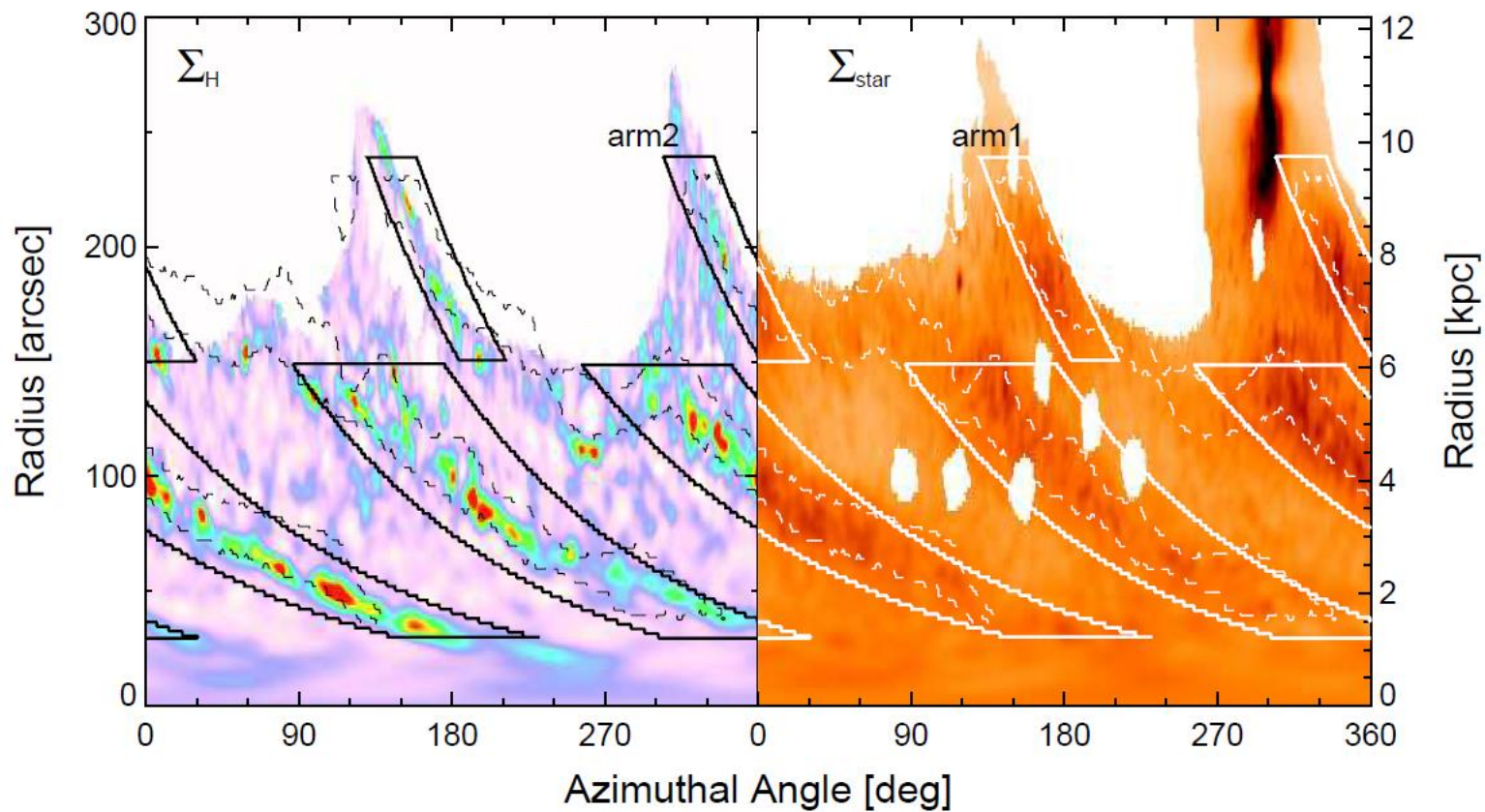


Figure 2. Phase diagrams of Σ_H (left) and Σ_{star} (right) of M51. Each image is normalized by its azimuthal average at each radius in order to emphasize the spiral arm structure. Thin dashed contours indicate the arm definition by Egusa et al. (2013), while thick solid contours indicate new definition adopted in this paper (see §2.4).

Разрешение – 6'' (240 pc)

	arm2	18.8 ± 0.6	23.4 ± 0.9
outer arms: $r = 151'' - 220''$			
		gas	star
arm1		27.8 ^{+1.3} _{-1.2}	37.4 ^{+3.5} _{-3.0}
arm2		27.6 ^{+1.5} _{-1.4}	32.4 ^{+2.8} _{-2.4}

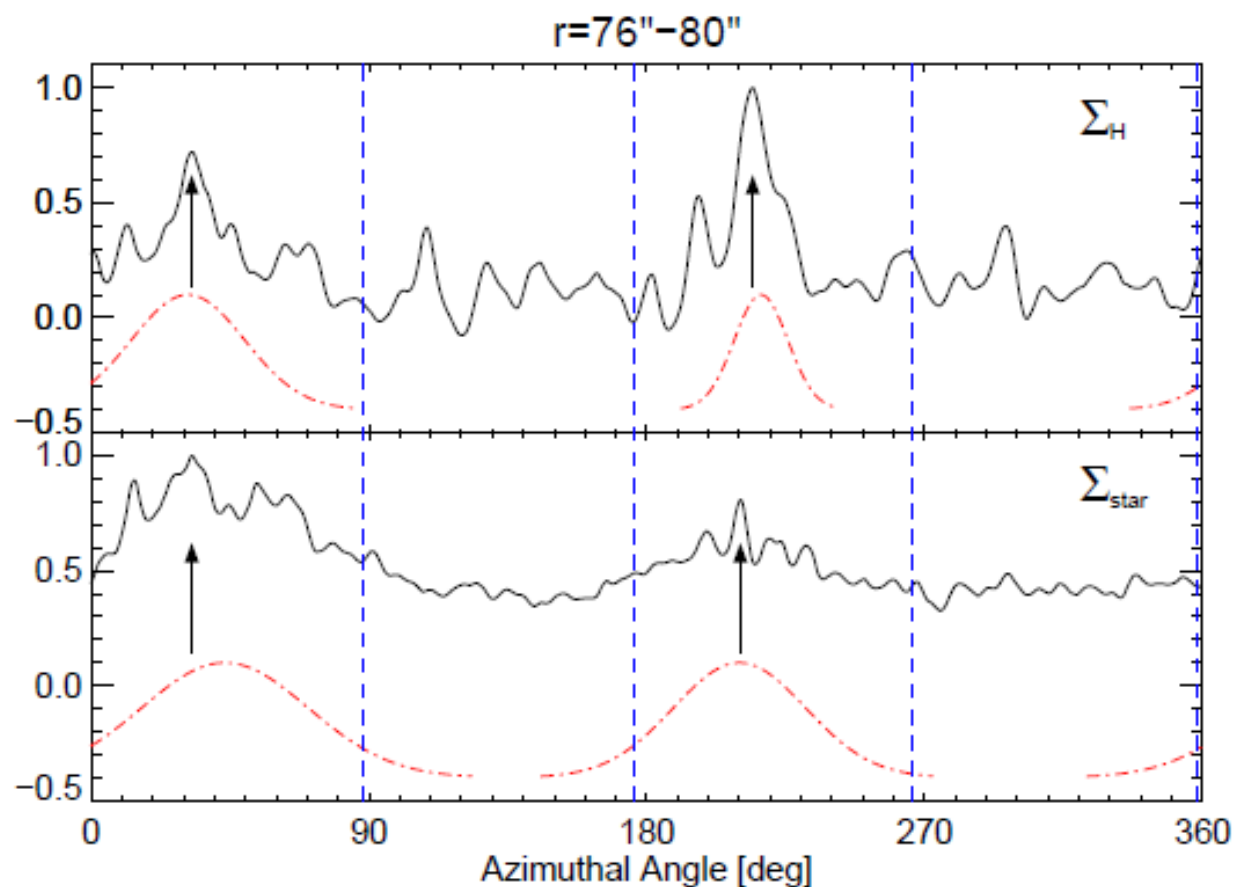


Figure 3. Azimuthal profiles of Σ_H (top) and Σ_{star} (bottom) at a radial bin of $r = 76''-80''$. The vertical axis is in arbitrary unit. Arrows indicate the position of identified peaks and blue dashed vertical lines indicate the boundary of arm regions at this radius. Fitted gaussian profiles are presented by red dashed-dotted lines.

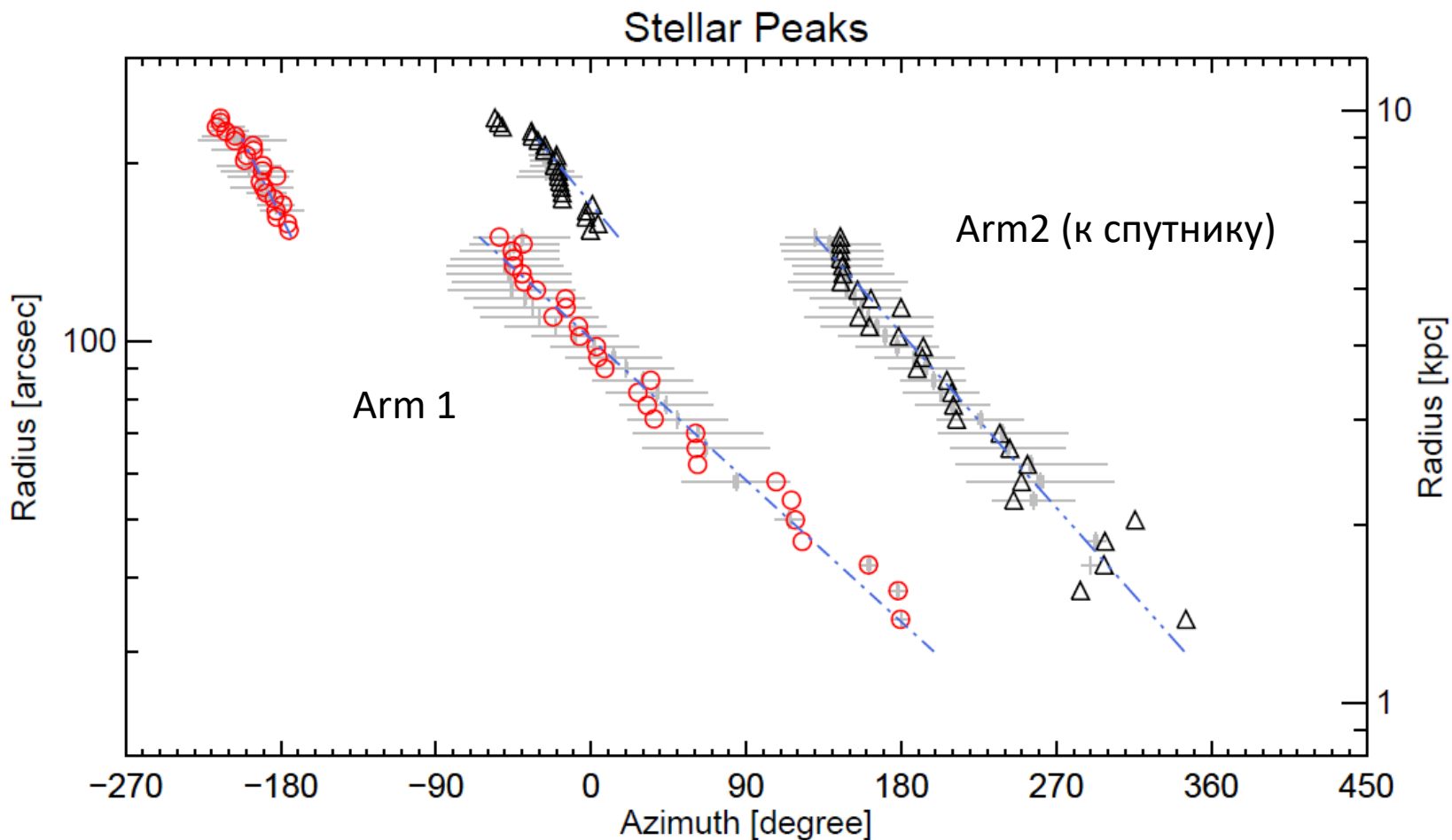
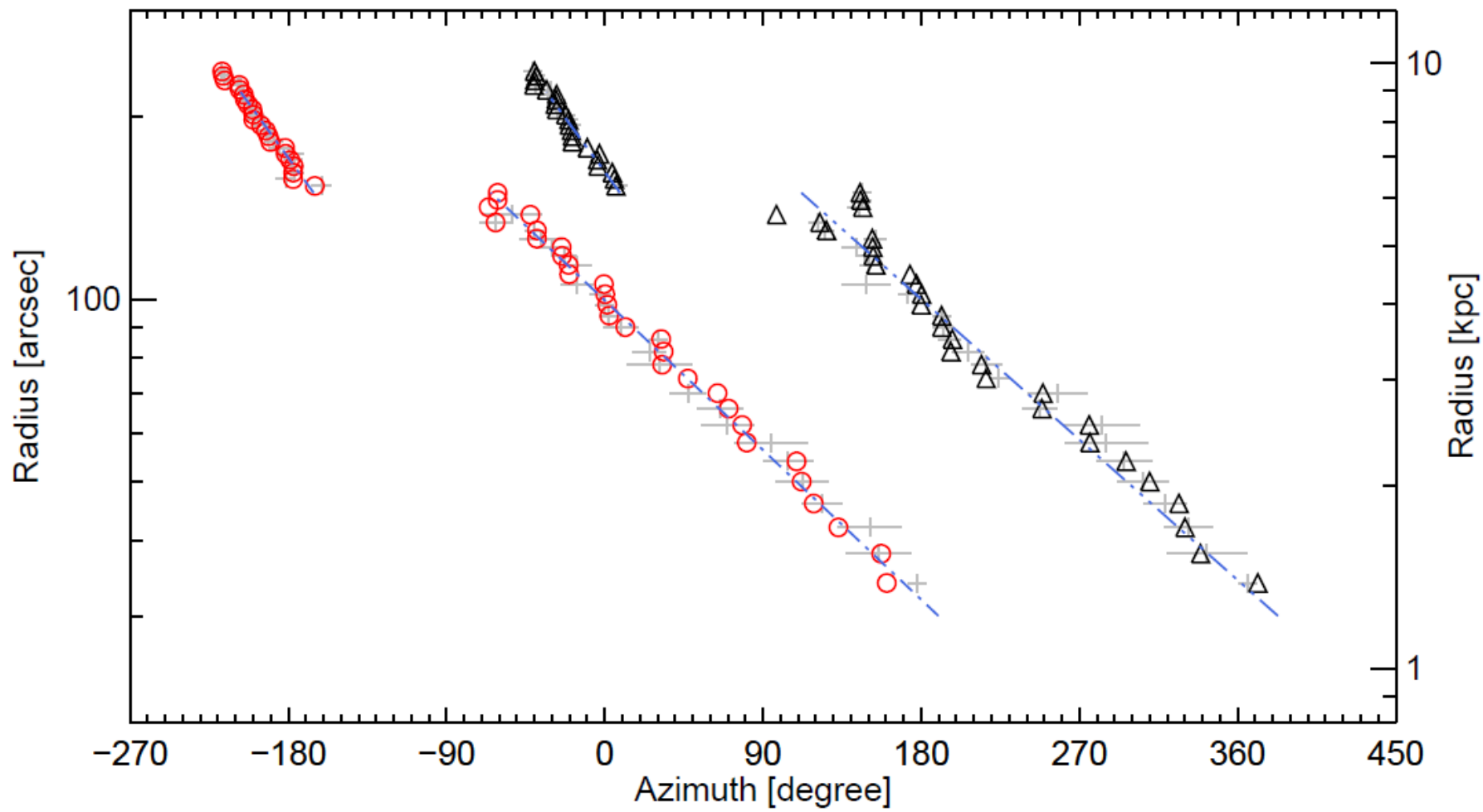
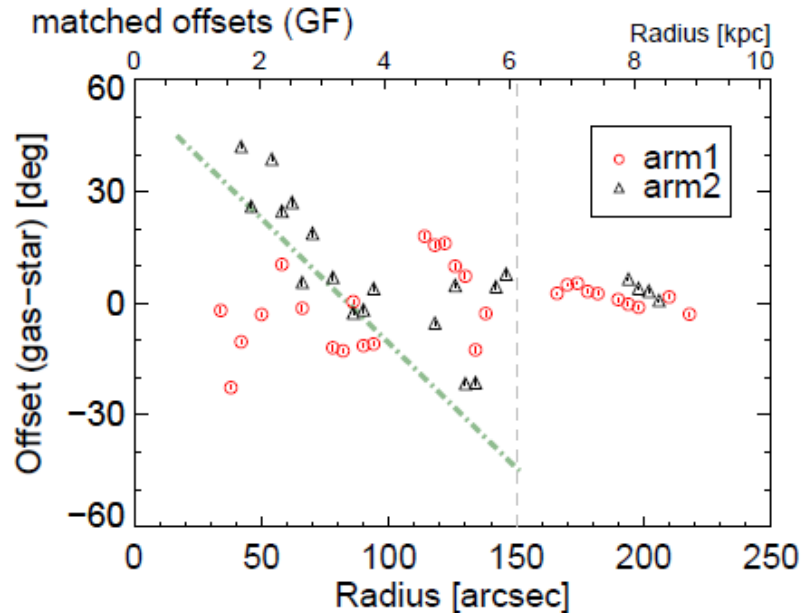
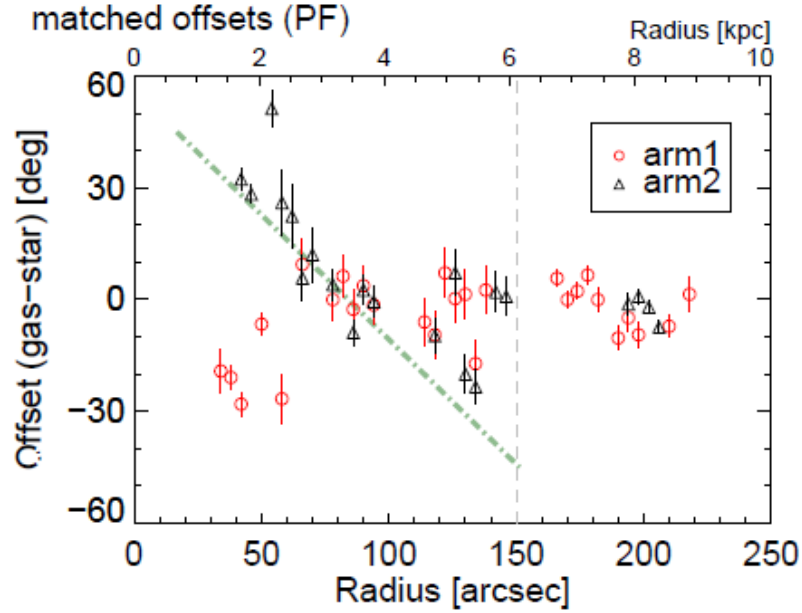


Figure 4. Location of gas (top) and stellar (bottom) spiral arms by different methods. Red circles and black triangles are peaks of azimuthal profiles within the arm regions. Blue dot-dashed lines are logarithmic spiral arms fitted to these peaks. Gray crosses indicate peak positions from the gaussian fit. Thin horizontal bars indicate the width ($\pm\sigma$) of a fitted gaussian profile. Thick bars indicate the uncertainty of the peak but they are generally too small to be visible in this plot. Gauss-fit peaks outside the arm regions are excluded.

Gas Peaks



Results



Сдвиги между максимумами распределений на каждом R.

Выводы.

- Для внешних ветвей данные ненадежны. Прямых свидетельств волны плотности нет.

Для внутренних ветвей:

- Ветвь 1 (не показывает волновых свойств, хотя Egusa et al. (2009) нашли CO-H α offsets соответствующий $t_{SF} = 7.1 \pm 0.5$ Myr,. Получается, относительное движение газа и звезд есть, ударная волна есть, но постоянной угловой скорости у структуры нет. Медленная закрутка.
- Ветвь 2 (к спутнику) показывает все признаки волны плотности с радиусом коротации 150'' (6 кпс).